Crystal structure of oxybutynin hydrochloride hemihydrate, $C_{22}H_{32}NO_3Cl(H_2O)_{0.5}$

James A. Kaduk,[1,2,a] Nicholas C. Boaz,[2] Amy M. Gindhart,[3] and Thomas N. Blanton[3]
[1]*Illinois Institute of Technology, 3101 S. Dearborn St., Chicago, Illinois 60616*
[2]*North Central College, 131 S. Loomis St., Naperville, Illinois 60540*
[3]*ICDD, 12 Campus Blvd., Newtown Square, Pennsylvania 19073-3273*

(Received 2 August 2018; accepted 24 October 2018)

The crystal structure of oxybutynin hydrochloride hemihydrate has been solved and refined using synchrotron X-ray powder diffraction data, and optimized using density functional techniques. Oxybutynin hydrochloride hemihydrate crystallizes in space group *I*2/*a* (#15) with $a = 14.57266(8)$, $b = 8.18550(6)$, $c = 37.16842(26)$ Å, $\beta = 91.8708(4)°$, $V = 4421.25(7)$ Å^3, and $Z = 8$. The compound exhibits X-ray-induced photoreduction of the triple bond. Prominent in the layered crystal structure is the N–H···Cl hydrogen bond between the cation and anion, as well as O–H···Cl hydrogen bonds from the water molecule and hydroxyl group of the oxybutynin cation. C–H···Cl hydrogen bonds also contribute to the crystal energy, and help determine the conformation of the cation. The powder pattern is included in the Powder Diffraction File™ as entry 00-068-1305. © *2019 International Centre for Diffraction Data*. [doi:10.1017/S0885715618000842]

Key words: oxybutynin hydrochloride, Ditropan, powder diffraction, Rietveld refinement, density functional theory

I. INTRODUCTION

Oxybutynin hydrochloride (brand names Cystrin, Ditropan, Dridase, Kentera, Pollakisu, Tropax, and others) is used for the treatment of urinary incontinence. Oxybutyin hydrochloride belongs in the class of antispasmodics and works by relaxing the bladder muscles and reducing urination urge and frequency. The systematic name (CAS Registry number 1508-65-2) is 4-diethylamino-2-butynyl-phenylcyclohexylglycolate hydrochloride. A two-dimensional molecular diagram of oxybutynin hydrochloride is shown in Figure 1.

Powder data for oxybutynin free base are reported in Ray *et al*. (2013). A powder pattern for oxybutynin hydrochloride is contained in Nakamichi *et al*. (1997). The powder pattern and other physical properties of (*S*)-oxybutynin hydrochloride are reported in Luner *et al*. (2001).

This work was carried out as part of a project (Kaduk *et al*., 2014) to determine the crystal structures of large-volume commercial pharmaceuticals, and include high-quality powder diffraction data for them in the Powder Diffraction File (Fawcett *et al*., 2017).

II. EXPERIMENTAL

Oxybutynin hydrochloride was a commercial regent, purchased from United States Pharmacopeial Convention (Lot #R039X0), and was used as-received. The white powder was packed into a 1.5 mm diameter Kapton capillary, and rotated during the measurement at ~50 Hz. The powder pattern was measured at 295 K at beam line 11-BM (Lee *et al*., 2008; Wang *et al*., 2008) of the Advanced Photon Source at Argonne National Laboratory using a wavelength of 0.457667 Å from 0.5–50°2θ with a step size of 0.001° and a counting time of 0.1 s/step. The beamline staff indicated that the sample showed some beam damage, with the strongest peaks shifting to lower angles and getting slightly broader. The pattern was difficult to index, ultimately because we did not search for large-enough unit cells. The successful strategy was to use DICVOL (Louër and Boultif, 2007) as incorporated into FOX (Favre-Nicolin and Černý, 2002), with the options of "weak diffraction" and "centered cells". The pattern was indexed on a body-centered monoclinic unit cell having $a = 14.571$, $b = 8.186$, $c = 37.157$ Å, $\beta = 91.89°$, $V = 4429$ Å^3, and $Z = 8$. Analysis of the systematic absences suggested the space group *I*2/*a,* which was confirmed by successful solution and refinement of the structure. A reduced cell search in the Cambridge Structural Database (Groom *et al*., 2016) combined with the chemistry "C H N O only" yielded 30 hits, but no structure containing oxybutynin.

An oxybutynin cation was built using Spartan '16 (Wavefunction, 2017), and its equilibrium conformation determined. The resulting .mol2 file was converted into a Fenske-Hall *Z*-matrix file using OpenBabel (O'Boyle *et al*., 2011). The structure was solved using oxybutynin and Cl fragments with both FOX (Favre-Nicolin and Černý, 2002) and DASH (David *et al*., 2006); both programs yielded the identical structure. The structure contained a void on a twofold axis, positioned ideally to be occupied by a water molecule acting as a hydrogen bond donor to two chloride anions. The structure was also solved by direct methods using EXPO2014 (Altomare *et al*., 2013). Although default direct methods were not successful, application of the COVMAP option to all 20 solutions yielded (in ~8 h of computing time) the

[a]Author to whom correspondence should be addressed. Electronic mail: kaduk@polycrystallography.com

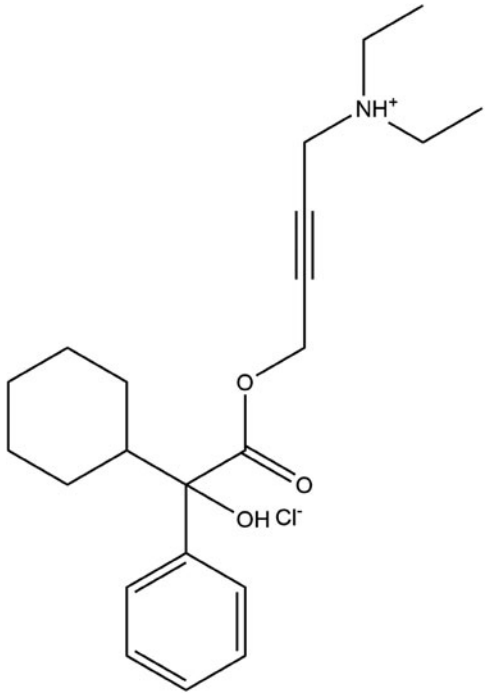

Figure 1. The molecular structure of oxybutynin hydrochloride.

complete structure, including the oxygen atom of the water molecule. Despite no mention in the literature, oxybutynin hydrochloride crystallizes as a hemihydrate.

Thermogravimetric analysis indicated that the sample contained 1.2 wt% water, instead of the 2.2% expected from the hemihydrate. Perhaps the hydrate is non-stoichiometric, though the crystallography indicates full occupancy. Analysis using ^{1}H and ^{13}C NMR of oxybutynin hydrochloride was used to verify the structure of the molecule. Spectra were acquired on a Bruker Avance III HD spectrometer as a solution in dimethyl sulfoxide-d_6 at 400 and 101 MHz for the ^{1}H and ^{13}C spectra, respectively. Assignment of the ^{13}C spectrum was performed using two-dimensional HSQC and HSQC-TOCSY experiments.

Rietveld refinement was carried out using GSAS (Toby, 2001; Larson and Von Dreele, 2004). Only the 1.0–27.0° 2θ portion of the pattern was included in the refinement (d_{min} = 0.980 Å), with an excluded region 1.5–2.0° 2θ to eliminate a relatively sharp peak from the Kapton capillary. All non-H bond distances and angles were subjected to restraints, based on a Mercury/Mogul Geometry Check (Bruno *et al*., 2004; Sykes *et al*., 2011) of the molecule. The Mogul average and standard deviation for each quantity were used as the restraint parameters. The phenyl ring C2–C7 was restrained to be planar. The restraints contributed 3.3% to the final χ^2. The U_{iso} of the non-H atoms were grouped by chemical similarity. The U_{iso} of each hydrogen atom was fixed at 1.3× that of the heavy atom to which it was attached. The peak profiles were described using profile function #4 (Thompson *et al*., 1987; Finger *et al*., 1994), which includes the Stephens (1999) anisotropic strain broadening model. The background was modeled using a three-term shifted Chebyshev polynomial, with a six-term diffuse scattering function to model the Kapton capillary and any amorphous component. The final refinement of 122 variables using 25602 observations (25539 data points and 63 restraints) yielded the residuals R_{wp} = 0.0909, R_p = 0.0720, and χ^2 = 3.251. The largest peak (1.52 Å from H52) and hole (1.04 Å from H53) in the difference Fourier map were 0.57 and −0.54 eÅ^{-3}, respectively, and occur in one of the ethyl groups. The Rietveld plot is included as Figure 2. The largest errors in the fit are in the positions and shapes of some of the low-angle peaks, and probably reflect specimen damage.

Although the statistical and graphical residuals were reasonable, examining the geometry of the refined molecule showed that it was unusual. The C37–C38 triple bond distance refined to 1.357 Å instead of the expected 1.19 Å, and the C34–C37–C38 angle was 135.1° instead of the

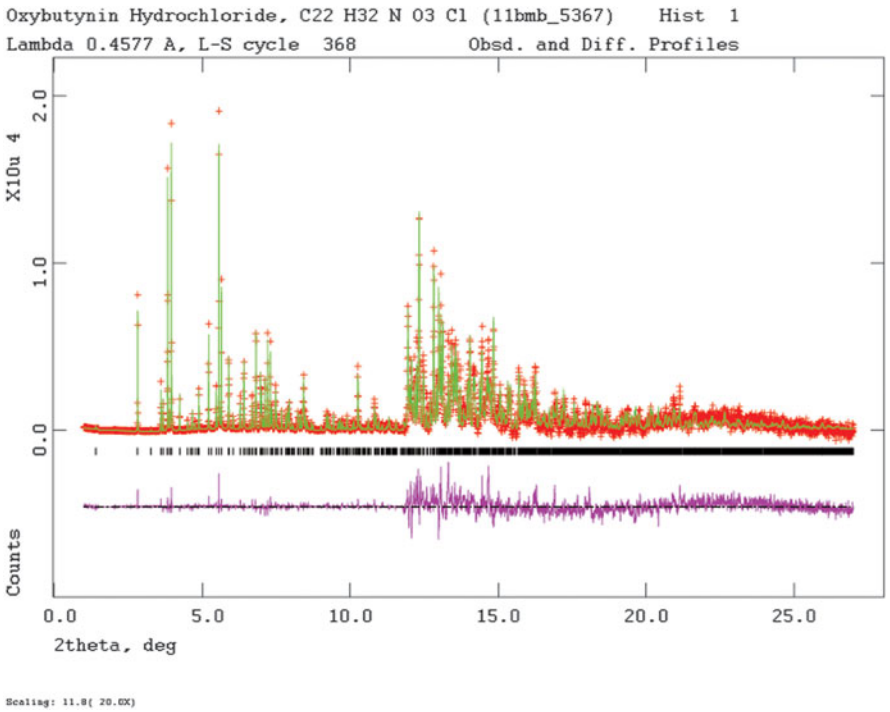

Figure 2. (Color online) The Rietveld plot for the refinement of oxybutynin hydrochloride hemihydrate. The red crosses represent the observed data points, and the green line is the calculated pattern. The magenta curve is the difference pattern, plotted at the same vertical scale as the other patterns. The row of black tick marks indicates the calculated reflection positions. The vertical scale has been multiplied by a factor of 20 for 2θ>11.8°.

https://doi.org/10.1017/S0885715618000842 Published online by Cambridge University Press

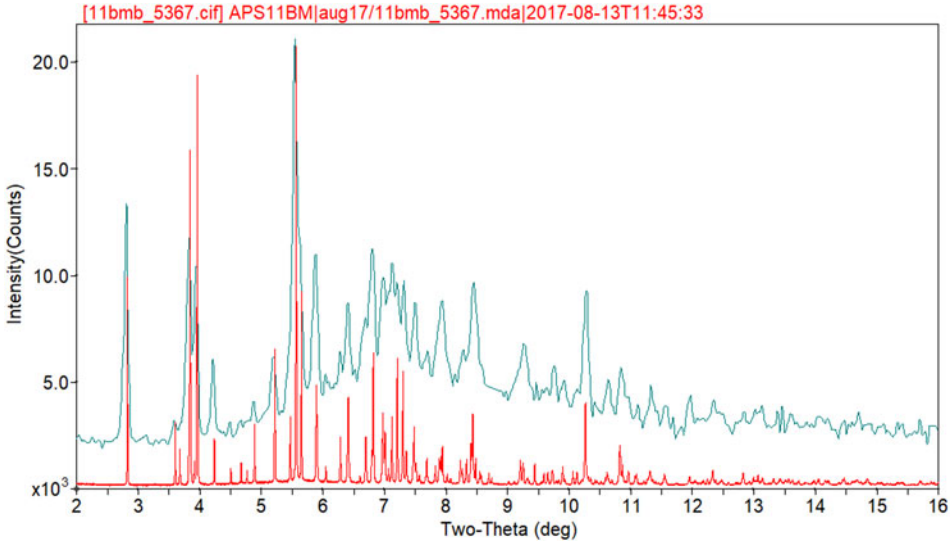

Figure 3. (Color online) Comparison of the synchrotron powder diffraction pattern to the laboratory X-ray powder diffraction pattern of European Patent 0580860 B1 (Nakamichi *et al*., 1997; Nippon Shinyaku). The literature pattern (measured using Cu*Kα* radiation) was digitized using UN-SCAN-IT (Silk Scientific, 2013), and re-scaled to the synchrotron wavelength of 0.457667 Å using Jade 9.8 (MDI, 2017).

expected 173°. Both of these features suggested that the triple bond has (at least partially) been hydrogenated to a double bond. Re-starting the refinement from the DFT-optimized structured yielded the same "bent" molecule. The same "bent" structure was obtained from a refinement using laboratory Mo*Kα* data. NMR analysis indicates that the sample used for diffraction did initially contain a triple bond at the C37–38 position. Specifically, as shown in Figure 4, the

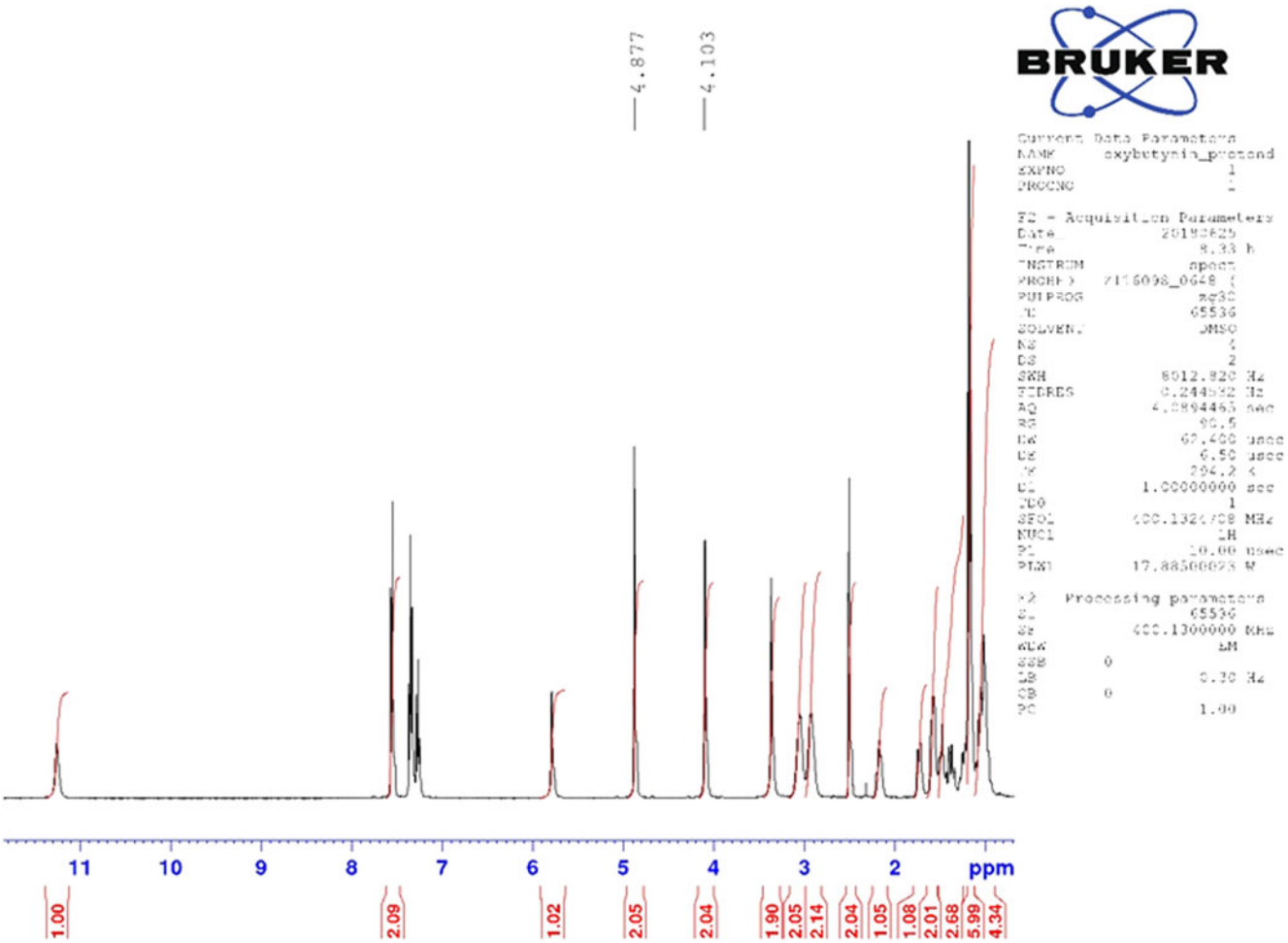

Figure 4. (Color online) ^{1}H NMR (400 MHz, DMSO-d_6) spectrum of oxybutynin hydrochloride. The un-split resonances at 4.9 and 4.1 ppm arise from the protons on C34 and C39, respectively.

https://doi.org/10.1017/S0885715618000842 Published online by Cambridge University Press

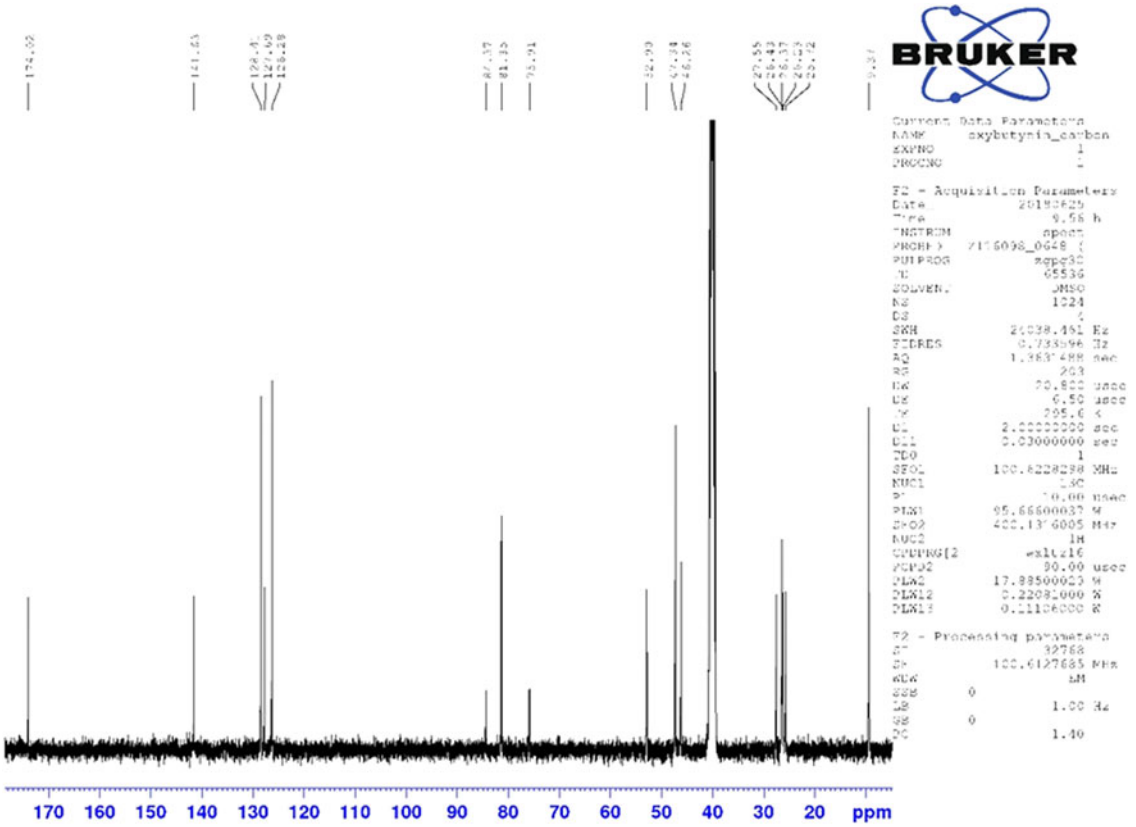

Figure 5. (Color online) ^{13}C NMR (101 MHz, DMSO-d_6) spectrum of oxybutynin hydrochloride. The resonances at 84.3 and 75.9 ppm arise from the C37 and C38 triple bond. These assignments were made using a two-dimensional HSQC-TOCSY experiment.

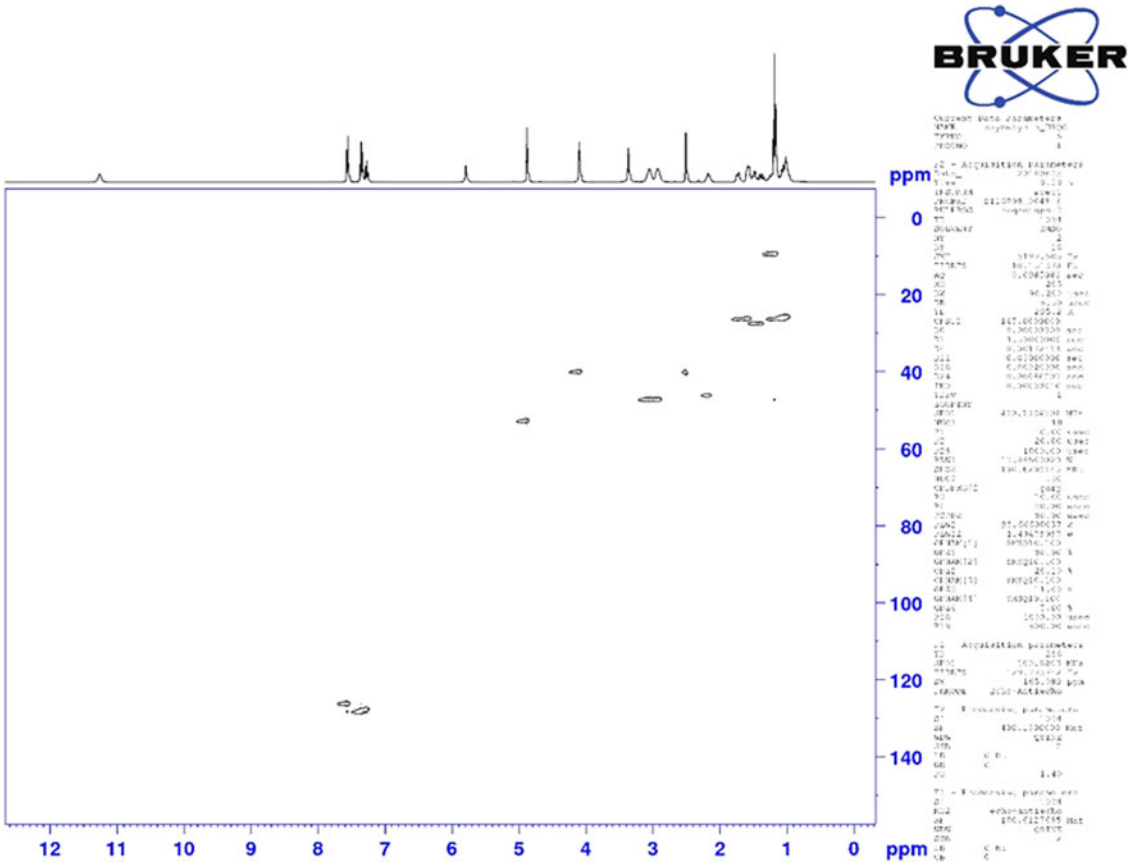

Figure 6. (Color online) Two-dimensional HSQC NMR spectrum of oxybutynin (DMSO-d_6) used to assign the ^{13}C resonances of C34 and C39.

https://doi.org/10.1017/S0885715618000842 Published online by Cambridge University Press

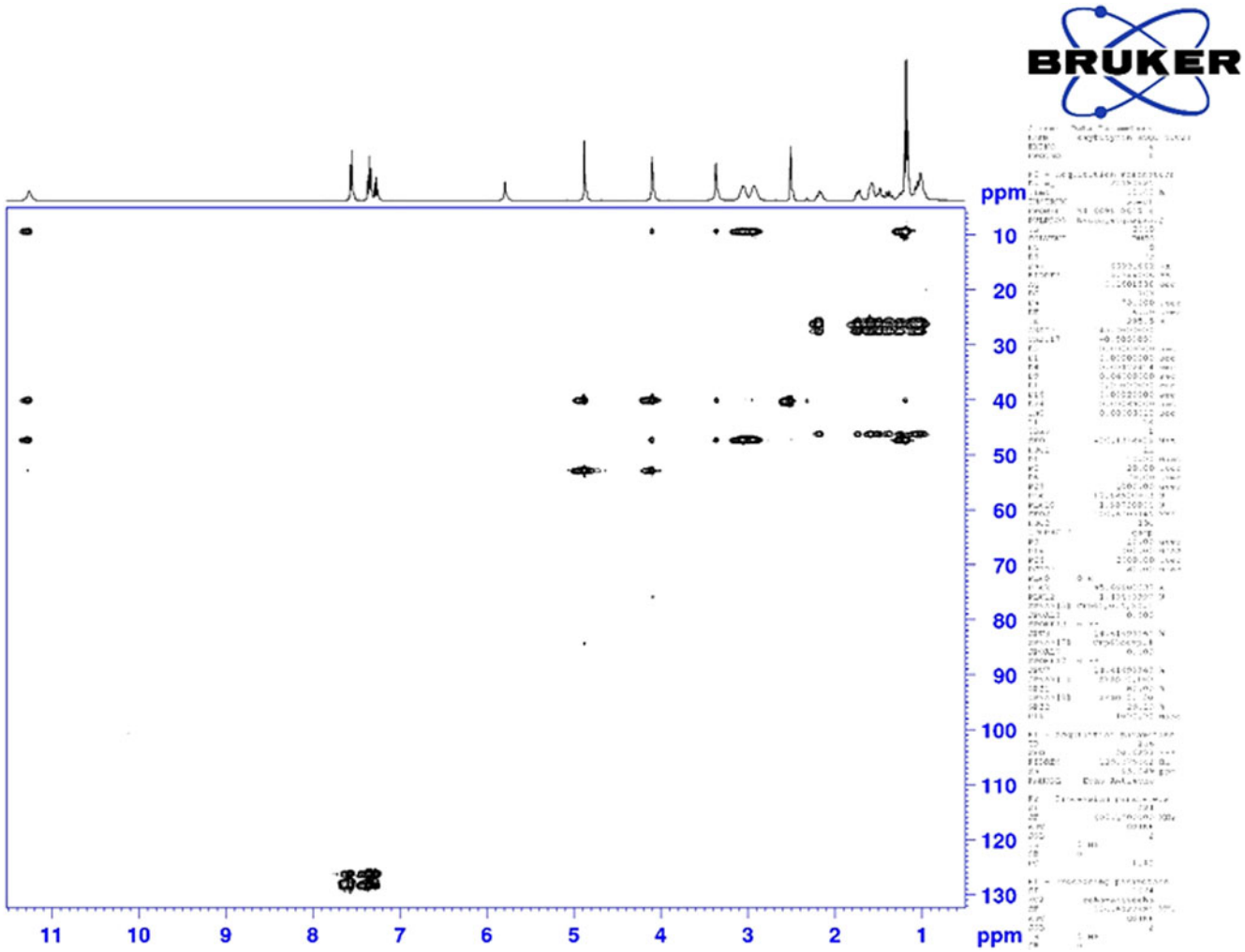

Figure 7. (Color online) Two-dimensional HSQC-TOCSY NMR spectrum of oxybutynin (DMSO-d_6) used to assign the ^{13}C resonances of C37 and C38.

^{1}H NMR resonances of the protons on C34 and C39 which are adjacent to the C37–38 triple bond (at 4.88 and 4.10 ppm, respectively) are unsplit, indicating a lack of coupled proton neighbors. Additionally, the chemical shifts of these resonances are typical for methylene groups adjacent to both a triple bond and an electronegative heteroatom. Moreover, the ^{13}C NMR spectrum, as shown in Figure 5 shows the resonances of C37 and C38 (84.3 and 75.9 ppm, respectively) are typical for those of alkynes. The identity of the carbon resonances for C37 and C38 was determined using two-dimensional HSQC and HSQC-TOCSY experiments (Figures 6 and 7).

Density functional geometry optimizations (fixed experimental unit cell) were carried out using CRYSTAL14 (Dovesi *et al*., 2014), both for the expected molecule and the photoreduced version. The basis sets for the H, C, N, O, and Cl atoms were those of Peintinger *et al*. (2013). The calculations were run on eight 2.1 GHz Xeon cores (each with 6 GB RAM) of a 304-core Dell Linux cluster at IIT, used 8 *k*-points and the B3LYP functional, and took ~9 and 5 days, respectively.

III. RESULTS AND DISCUSSION

The powder pattern of oxybutynin hydrochloride hemihydrate is similar enough to that of "oxybutynin hydrochloride" from Nakamichi *et al*. (1997) to conclude that they are the same substance (Figure 3). We have not found in the literature a mention that this compound is a hemihydrate. As expected, the powder pattern of the (*S*) enantiomorph reported by Luner *et al*. (2001) is very different from that of racemic oxybutynin hydrochloride hemihydrate reported here. The refined atom coordinates of oxybutynin hydrochloride hemihydrate and the coordinates from the DFT optimizations of the molecules containing a triple and a double

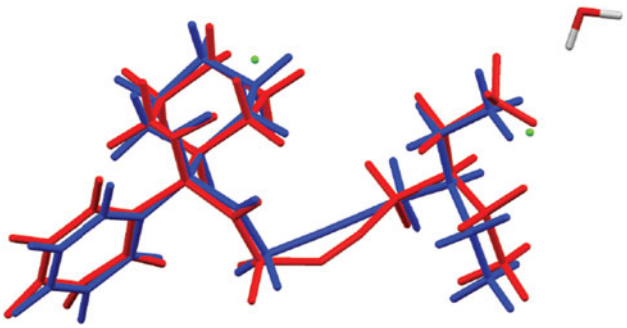

Figure 8. (Color online) Comparison of the refined and optimized structures of the cation in oxybutynin hydrochloride hemihydrate. The Rietveld refined structure is in red, and the DFT-optimized structure is in blue.

https://doi.org/10.1017/S0885715618000842 Published online by Cambridge University Press

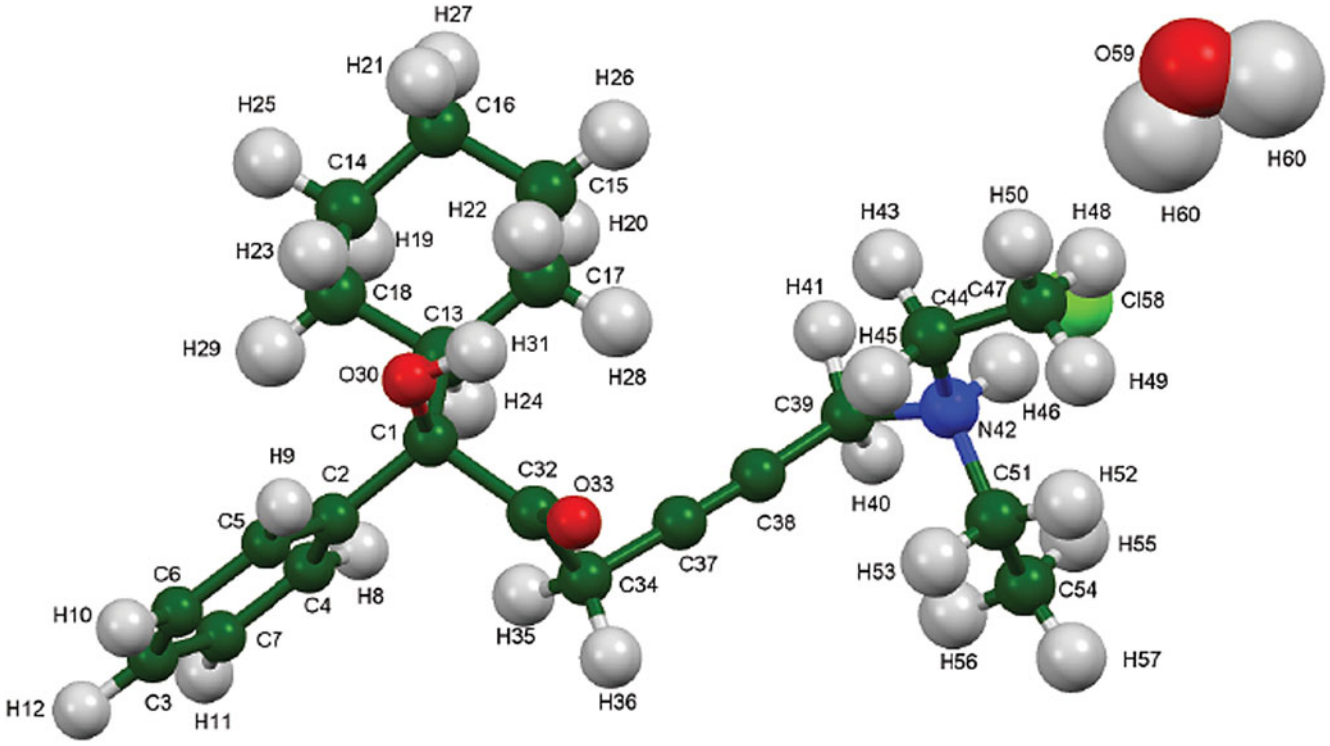

Figure 9. (Color online) The asymmetric unit of oxybutynin hydrochloride hemihydrate, with the atom numbering. The atoms are represented by 50% probability spheroids.

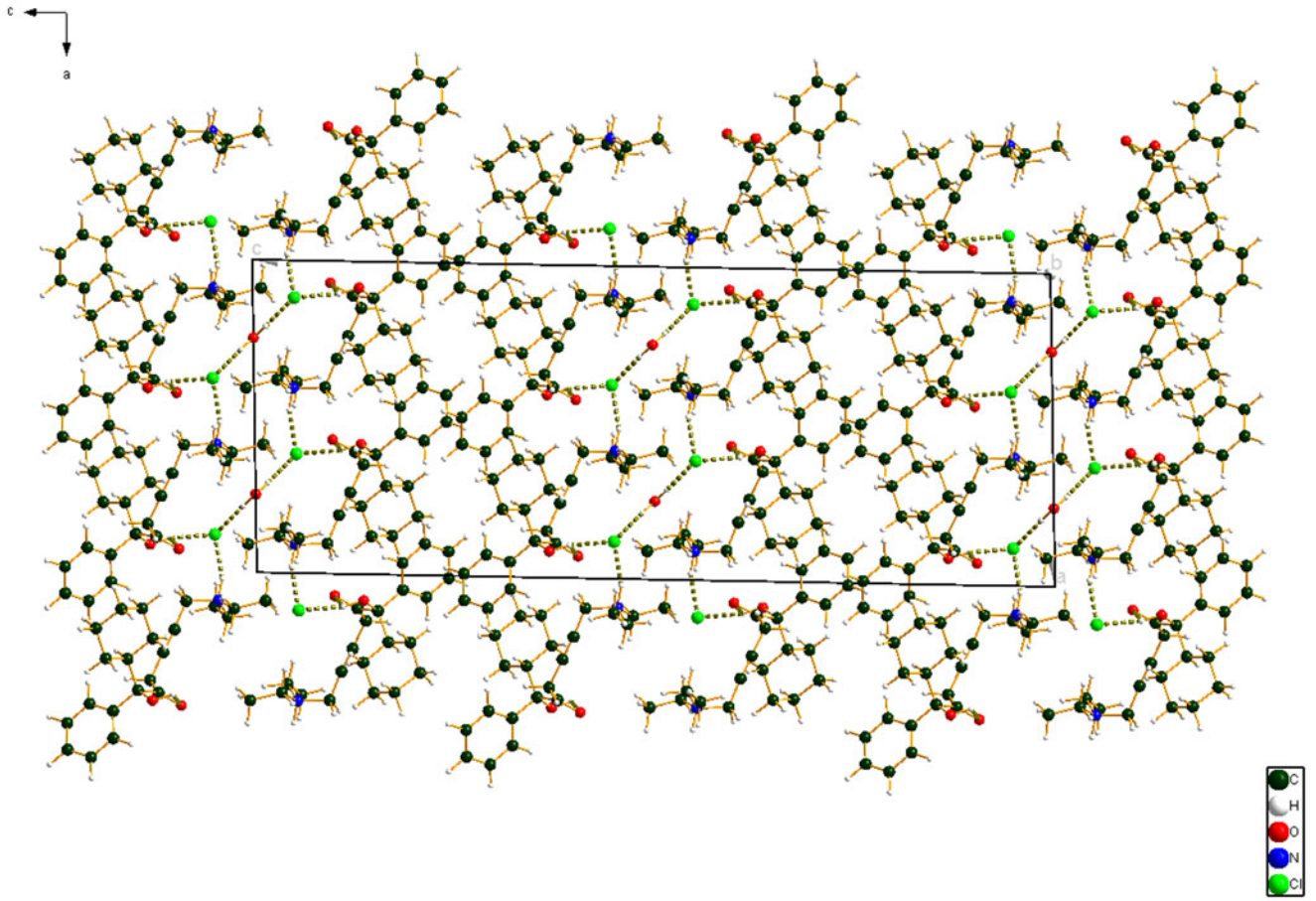

Figure 10. (Color online) The crystal structure of oxybutynin hydrochloride hemihydrate, viewed down the *b*-axis.

https://doi.org/10.1017/S0885715618000842 Published online by Cambridge University Press

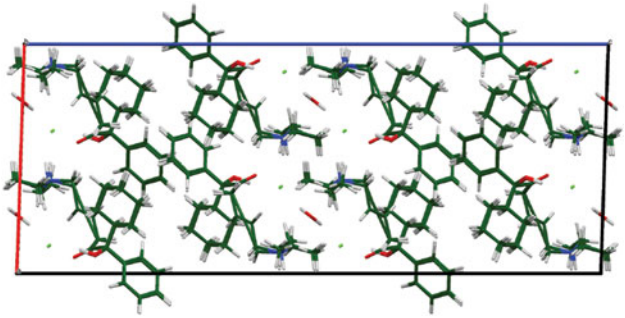

Figure 11. (Color online) The crystal structures of oxybutynin hydrochloride hemihydrate and its photoreduced version, viewed down the *b*-axis.

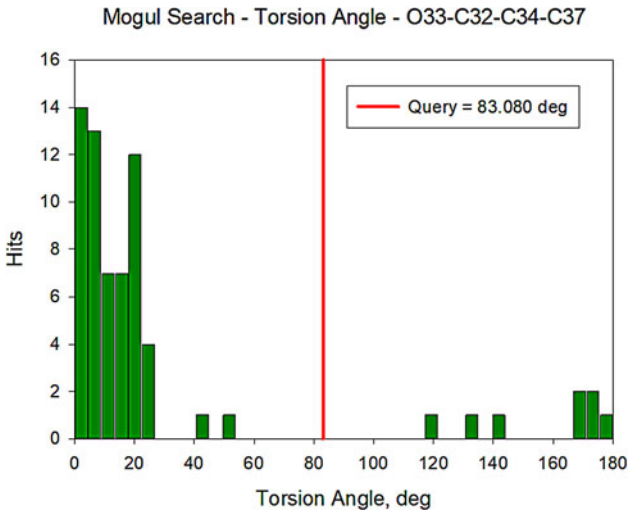

Figure 12. (Color online) Distribution of the O33–C32–C34–C37 torsion angles in the Cambridge Structural Database.

bond are reported in the CIFs attached as Supplementary Material. The root-mean-square Cartesian displacement of the non-hydrogen atoms in the oxybutynin cations is 0.363 Å (Figure 8). The largest deviation is 0.9080 Å at C37, the site of the apparent photoreduction. The agreement between the refined and optimized structures is at the upper end of the range of correct powder structures (van de Streek and Neumann, 2014), but the photoreduction complicates interpretation of this measure. This discussion uses the DFT-optimized structure. The asymmetric unit (with atom numbering) is illustrated in Figure 9, and the crystal structure is presented in Figure 10.

The DFT-optimized structures of oxybutynin hydrochloride hemihydrate and the photoreduced version are similar (Figure 11). The reduction of the triple bond is easily accommodated, with minimal displacements of the other atoms of the molecule.

All of the bond distances and bond angles fall within the normal ranges indicated by a Mercury Mogul Geometry check (Macrae *et al*., 2008). The torsion angles involving rotation of the C32–C34 bond are flagged as unusual, but they are not unprecedented; the O33–C32–C34–C37 torsion angle of 83.09° is compared with the Mogul distribution in Figure 12. There are few examples of the types of torsion angles which involve the two portions of the oxybutynin cation, so it may not be a surprise that unusual torsion angles are observed.

Quantum chemical geometry optimizations (DFT/B3LYP/6-31G*/water) using Spartan '16 (Wavefunction, 2017) indicated that the observed conformation of the oxybutynin cation is 9.8 kcal/mole higher in energy than the local minimum energy conformation. The rms Cartesian displacement is 1.078 Å, and there are many differences in conformation. Molecular mechanics conformational analysis indicated that the global minimum energy conformation (−1.9 kcal/mole) differs from the observed conformation by a 120° rotation of the cationic end of the molecule, and thus that intermolecular interactions are important in determining the solid-state conformation.

The cation–anion interactions and hydrogen bonds result in a double-layer structure, with the layers parallel to the *ab* plane. The layers are separated by hydrocarbon–hydrocarbon contacts. Analysis of the contributions to the total crystal energy using the Forcite module of Materials Studio (Dassault, 2018) suggests that angle, bond, and torsion distortion terms are significant in the intramolecular deformation energy. The intermolecular energy contains significant contributions from van der Waals attractions and electrostatic repulsions. In this force-field-based analysis, the electrostatic interactions include hydrogen bonds. The hydrogen bonds are better analyzed using the results of the DFT calculation.

As expected, the discrete N–H···Cl hydrogen bond between the cation and anion is prominent in the crystal structure (Table I). The Cl also acts as an acceptor in O–H···Cl hydrogen bonds, both from the water molecule and the hydroxyl group O30–H31. The energies of these hydrogen bonds were calculated according to the correlation developed in Kaduk (2002). The Cl apparently acts as an acceptor in three C–H···Cl interactions involving methylene and methyl groups. These interactions may contribute to the orientation of the cationic end of the oxybutynin. There also appears to be a C7–H11···C6 interaction between phenyl rings.

The volume enclosed by the Hirshfeld surface (Figure 13; Hirshfeld, 1977; McKinnon *et al*., 2004; Spackman and

TABLE I. Hydrogen bonds (CRYSTAL14) in oxybutynin hydrochloride hemihydrate.

H-bond	D–H, Å	H···A, Å	D····A, Å	D–H···A,°	Overlap, *e*	E, kcal/mol
N42–H46···Cl58	1.051	2.125	3.136	160.8	0.077	
O59–H60···Cl58	0.978	2.247	3.223	176.2	0.057	33.6
O30–H31···Cl58	0.983	2.241	3.172	157.7	0.052	32.1
C51–H52···Cl58	1.087	2.680	3.652	148.6	0.023	
C51–H53···Cl58	1.089	2.968	3.806	133.9	0.015	
C54–H55···Cl58	1.085	2.976	3.817	134.2	0.012	
C7–H11···C6	1.081	2.555	3.548	152.3	0.016	

https://doi.org/10.1017/S0885715618000842 Published online by Cambridge University Press

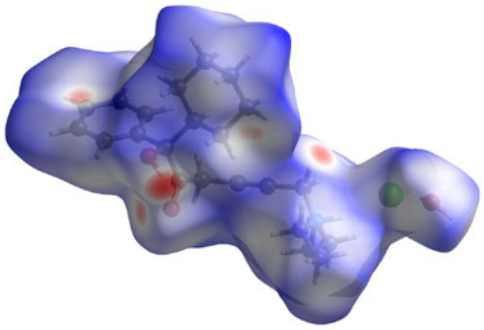

Figure 13. (Color online) The Hirshfeld surface of oxybutynin hydrochloride hemihydrate. Intermolecular contacts longer than the sums of the van der Waals radii are colored blue, and contacts shorter than the sums of the radii are colored red. Contacts equal to the sums of radii are white.

Jayatilaka, 2009; Wolff *et al.*, 2012) is 557.68 Å^3 (including a whole water molecule), 100.91% of 1/8 the unit-cell volume. The packing is thus fairly dense. All of the significant close contacts (red in Figure 13) involve the hydrogen bonds.

The Bravais–Friedel–Donnay–Harker (Bravais, 1866; Friedel, 1907; Donnay and Harker, 1937) morphology suggests that we might expect platy morphology for oxybutynin hydrochloride hemihydrate, with {002} as the principal faces. A fourth-order spherical harmonic preferred orientation model was included in the refinement; the texture index was 1.0067, indicating that preferred orientation was not significant in this rotated capillary specimen.

The powder pattern is included in the Powder Diffraction File™ as entry 00-068-1305.

SUPPLEMENTARY MATERIAL

The supplementary material for this article can be found at https://doi.org/10.1017/S0885715618000842.

Acknowledgements

Use of the Advanced Photon Source at Argonne National Laboratory was supported by the US Department of Energy, Office of Science, Office of Basic Energy Sciences, under Contract No. DE-AC02-06CH11357. This work was partially supported by the International Centre for Diffraction Data. The authors thank Lynn Ribaud and Saul Lapidus at 11-BM for their assistance in data collection, Andrey Rogachev for the use of computing resources at IIT, and Jose Orozco at IIT for the TGA analysis.

Altomare, A., Cuocci, C., Giacovazzo, C., Moliterni, A., Rizzi, R., Corriero, N., and Falcicchio, A. (**2013**). "EXPO2013: a kit of tools for phasing crystal structures from powder data," J. Appl. Crystallogr. **46**, 1231–1235.

Bravais, A. (**1866**). *Etudes Cristallographiques* (Gauthier Villars, Paris).

Bruno, I. J., Cole, J. C., Kessler, M., Luo, J., Motherwell, W. D. S., Purkis, L. H., Smith, B. R., Taylor, R., Cooper, R. I., Harris, S. E., and Orpen, A. G. (**2004**). "Retrieval of crystallographically-derived molecular geometry information," J. Chem. Inf. Sci. **44**, 2133–2144.

Dassault Systèmes (**2018**). *Materials Studio 2018* (BIOVIA, San Diego, CA).

David, W. I. F., Shankland, K., van de Streek, J., Pidcock, E., Motherwell, W. D. S., and Cole, J. C. (**2006**). "DASH: a program for crystal structure determination from powder diffraction data," J. Appl. Crystallogr. **39**, 910–915.

Donnay, J. D. H. and Harker, D. (**1937**). "A new law of crystal morphology extending the law of Bravais," Am. Mineral. **22**, 446–447.

Dovesi, R., Orlando, R., Erba, A., Zicovich-Wilson, C. M., Civalleri, B., Casassa, S., Maschio, L., Ferrabone, M., De La Pierre, M., D-Arco, P., Noël, Y., Causà, M., and Kirtman, B. (**2014**). "CRYSTAL14: A program for the ab initio investigation of crystalline solids," Int. J. Quantum Chem. **114**, 1287–1317.

Favre-Nicolin, V. and Černý, R. (**2002**). FOX, "Free objects for crystallography: a modular approach to ab initio structure determination from powder diffraction," J. Appl. Crystallogr. **35**, 734–743.

Fawcett, T. G., Kabekkodu, S. N., Blanton, J. R., and Blanton, T. N. (**2017**). "Chemical analysis by diffraction: the Powder Diffraction File™," Powder Diffr. **32**(2), 63–71.

Finger, L. W., Cox, D. E., and Jephcoat, A. P. (**1994**). "A correction for powder diffraction peak asymmetry due to axial divergence," J. Appl. Crystallogr. **27**(6), 892–900.

Friedel, G. (**1907**). "Etudes sur la loi de Bravais," Bull. Soc. Fr. Mineral. **30**, 326–455.

Groom, C. R., Bruno, I. J., Lightfoot, M. P., and Ward, S. C. (**2016**). "The Cambridge Structural Database," Acta Crystallogr. Sect. B: Struct. Sci., Cryst. Eng. Mater. **72**, 171–179.

Hirshfeld, F. L. (**1977**). "Bonded-atom fragments for describing molecular charge densities," Theor. Chem. Acta **44**, 129–138.

Kaduk, J. A. (**2002**). "Use of the Inorganic Crystal Structure Database as a problem solving tool", Acta Crystallogr. Sect. B: Struct. Sci. **58**, 370–379.

Kaduk, J. A., Crowder, C. E., Zhong, K., Fawcett, T. G., and Suchomel, M. R. (**2014**). "Crystal structure of atomoxetine hydrochloride (Strattera), $C_{17}H_{22}NOCl$," Powder Diffr. **29**(3), 269–273.

Larson, A. C. and Von Dreele, R. B. (**2004**). *General Structure Analysis System*, (*GSAS*), (Los Alamos National Laboratory Report LAUR 86–784).

Lee, P. L., Shu, D., Ramanathan, M., Preissner, C., Wang, J., Beno, M. A., Von Dreele, R. B., Ribaud, L., Kurtz, C., Antao, S. M., Jiao, X., and Toby, B. H. (**2008**). "A twelve-analyzer detector system for high-resolution powder diffraction," J. Synch. Rad. **15**(5), 427–432.

Louër, D. and Boultif, A. (**2007**). "Powder pattern indexing and the dichotomy algorithm," Zeitschrift Kristallogr. Suppl. **2007**, 191–196.

Luner, P. E., Kirsch, L. E., Majuru, S., Oh, E., Joshi, A. B., Wurster, D. A., and Redmon, M. P. (**2001**). "Preformulation studies on the S-isomer of oxybutynin hydrochloride, and Improved Chemical Entity (ICE™)," Drug. Devel. Ind. Pharm. **27**, 321–329.

Macrae, C. F., Bruno, I. J., Chisholm, J. A., Edington, P. R., McCabe, P., Pidcock, E., Rodriguez-Monge, L., Taylor, R., van de Streek, J., and Wood, P. A. (**2008**). "Mercury CSD 2.0 – new features for the visualization and investigation of crystal structures," J. Appl. Crystallogr. **41**, 466–470.

McKinnon, J. J., Spackman, M. A., and Mitchell, A. S. (**2004**). "Novel tools for visualizing and exploring intermolecular interactions in molecular crystals," Acta Crystallogr. Sect. B **60**, 627–668.

MDI (**2017**). *Jade 9.8* (Materials Data. Inc., Livermore, CA).

Nakamichi, K., Izumi, K., and Yasuura, H. (**1997**). "Method of Manufacturing Solid Dispersion," European Patent EP 0 580 860 B1.

O'Boyle, N., Banck, M., James, C. A., Morley, C., Vandermeersch, T., and Hutchison, G. R. (**2011**). "Open babel: an open chemical toolbox," J. Chem. Informatics **3**, 33.

Peintinger, M. F., Vilela Oliveira, D., and Bredow, T. (**2013**). "Consistent gaussian basis sets of triple-zeta valence with polarization quality for solid-state calculations," J. Comput. Chem. **34**, 451–459.

Ray, P. C., Sethi, M., Mahajan, S., and Tyagi, O. D. (Matrix Laboratories, Ltd.) (**2013**). "Crystalline Oxybutynin and Process for Preparing the Same," U.S. Patent 8,513,455.

Silk Scientific (**2013**). *UN-SCAN-IT 7.0* (Silk Scientific Corporation, Orem UT).

Spackman, M. A. and Jayatilaka, D. (**2009**). "Hirshfeld surface analysis," CrystEngComm **11**, 19–32.

Stephens, P. W. (**1999**). "Phenomenological model of anisotropic peak broadening in powder diffraction," J. Appl. Crystallogr. **32**, 281–289.

Sykes, R. A., McCabe, P., Allen, F. H., Battle, G. M., Bruno, I. J., and Wood, P. A. (**2011**). "New software for statistical analysis of Cambridge Structural Database data," J. Appl. Crystallogr. **44**, 882–886.

Thompson, P., Cox, D. E., and Hastings, J. B. (**1987**). "Rietveld refinement of Debye-Scherrer synchrotron X-ray data from Al_2O_3," J. Appl. Crystallogr. **20**(2), 79–83.

Toby, B. H. (**2001**). "EXPGUI, a graphical user interface for GSAS," J. Appl. Crystallogr. **34**, 210–213.
van de Streek, J. and Neumann, M. A. (**2014**). "Validation of molecular crystal structures from powder diffraction data with dispersion-corrected density functional theory (DFT-D)," Acta Crystallogr. Sect. B: Struct. Sci., Cryst. Eng. Mater. **70**(6), 1020–1032.
Wang, J., Toby, B. H., Lee, P. L., Ribaud, L., Antao, S. M., Kurtz, C., Ramanathan, M., Von Dreele, R. B., and Beno, M. A. (**2008**). "A dedicated powder diffraction beamline at the advanced photon source: commissioning and early operational results," Rev. Sci. Inst. **79**, 085105.
Wavefunction, Inc. (**2017**). Spartan '16 Version 2.0.3, Wavefunction Inc., 18401 Von Karman Ave., Suite 370, Irvine CA 92612.
Wolff, S. K., Grimwood, D. J., McKinnon, M. J., Turner, M. J., Jayatilaka, D., and Spackman, M. A. (**2012**). *CrystalExplorer Version 3.1* (University of Western Australia).

https://doi.org/10.1017/S0885715618000842 Published online by Cambridge University Press